Transworld Research Network
37/661 (2), Fort P.O.
Trivandrum-695 023
Kerala, India

Thermal Wave Physics and Related Photothermal Techniques: Basic Principles and Recent Developments, 2009: 159-190 ISBN: 978-81-7895-401-1 Editor: Ernesto Marín Moares

6. Characterization of semiconductors using photoacoustics

E. Marín[1], A. Calderón[1] and I. Riech[2]

[1]*Centro de Investigación en Ciencia Aplicada y Tecnología Avanzada, Legaria 694 Colonia Irrigación C.P. 11500, México D.F., México;* [2]*Facultad de Ingeniería Universidad Autónoma de Yucatán, Apdo. Postal 150 Cordemex Mérida, Yucatán, México*

Abstract. Since the early seventies, photoacoustic has been emerged as a well suited technique for the measurement of optical and transport properties of semiconductors, showing in many cases considerable advantages respecting other characterization methods. As these materials are often grown in the form of thin films on different kind of substrates, in this chapter we shall describe some of the theoretical models devised in the last years to the measurement of their electronic transport properties. We will also show how photoacoustic spectroscopy allows the measurement of the wavelength dependence of the optical absorption coefficient of very opaque semiconductor thin layers.

1. Introduction

Since the later fifties the field of semiconductors has become an enormous impact in society and global economy because semiconductor devices are the basis of some of the largest industries in the world, namely the micro- and optoelectronic industries, as well as of those depending on their products. One

Correspondence/Reprint request: Dr. E. Marín, Centro de Investigación en Ciencia Aplicada y Tecnología Avanzada Legaria 694, Colonia Irrigación, C.P. 11500, México D.F., México. E-mail: emarinm@ipn.mx

of the aims of semiconductor technology is to purify a material as much as possible and then to introduce impurities in a controlled manner in order to change their properties for specific applications, for example those describing the optical behavior and the transport characteristics of the electrical current carriers, i.e., electrons and holes, such as their recombination lifetimes and surface recombination velocity, as well as thermal transport properties, which play an important role in device performance. The conventional methods that have been used to evaluate these parameters [1] have some limitations: Electrical techniques are in general destructive or need special preparation of samples to make convinced measurements, for example by electrical contact deposition and thermal treatments, and optical techniques such as photoluminescence give mainly qualitative information about semiconductor material quality. It is highly desirable to conduct measurements of material properties without destroying it. Therefore, there is a great need for non-destructive methods which would enable us to measure as many semiconductor parameters as possible.

Since the rediscovering of the related effect in the 1970s by Rosencwaig [2, 3], the photoacoustic (PA) technique [4], and in general the photothermal (PT) methods, have been emerged as valuable and non-invasive tools for that purpose. For details of some early works about applications of PT techniques in the field of semiconductors the reader can be refereed to some of the existing reviews [5, 6].

However, a deep look at the literature shows that the majority of the published works deal with bulk materials. Taking into account that there has been a steadily decreasing trend in the interest of bulk semiconductor properties (a rather mature area of research) and that recent advances in crystal growth techniques have stimulated the attention on thin films or layers whose properties can differs in many cases from those of the corresponding volumetric materials, it is one of the aims of this chapter to review some of the existing applications related to their characterization by photoacoustics. Respecting optical characterization there is a great number of works related to photoacoustic spectroscopy (PAS) of bulk semiconductors and heterostructures using both, microphone and piezoelectric detection. However, only a few attempts have been devoted to the measurement of the wavelength dependence of the optical absorption coefficient of highly opaque semiconductor thin films. In many cases this parameter is very difficult to determine by conventional optical techniques because nearly full absorption of light should occur in the wavelength range of interest. As the knowledge of this parameter is very important (for example, in solar cells the optimum layer thicknesses for high efficiency devices depends on its value) various electrical methods have been reported in the literature for its measurement,

but they involve several approximations and the knowledge of some minority carrier related electronic parameters, reducing their application in general way [7]. For this reason we will describe some recent applications in this field showing the possibilities of PAS. Finally, as porous silicon layers grown on substrates of the same material are of interest since its discovery in the 1990s [8] due to their potential applications in optoelectronic devices and sensors [9] we will also comment about existing applications of the PA effect for their characterization.

In this article, we will limit our analysis to the case of harmonic periodical excitation because the pulsed techniques present several difficulties compared to those in the frequency domain and they were therefore applied only in a few cases for measurement of optical and transport properties [10]. Harmonic modulation takes also advantage of the excellent detection of low signal to noise ratio signals provided by Lock-in detection. In particular we will pay our attention to the PA method due to the following reason: PT techniques can be divided into direct contact (between sample and thermal wave's detector) and indirect contact methodologies. In the former case a thermal wave is produced in a sample where an excitation beam is absorbed, which is typically measured by a piezoelectric or a pyroelectric transducer bonded to the sample. In indirect techniques there is not mechanical contact between the sample and the sensor. This is the case in the microphone based PA method, where an acoustic wave is generated in a coupling medium adjacent to a sample to be analyzed, e.g. via a "thermal piston" effect [3], resulting in a heating of an air column in contact with the sample which leads to a measurable pressure fluctuation. Then, the inherent advantage of this indirect PA technique is that it is non-invasive compared with direct contact methods. Remote sensing techniques, such as PT radiometry [11], modulated photoreflectance [12], and those based in measurement of surface displacement [13] and gradient index modulation (thermal lens and mirage technique) [14, 15] are also non invasive, as the coupling medium is also generally air. Although some of them have been used in the past [5, 16-19], the most widely used technique in the field of semiconductors is the PA one, and the majority of the authors (see later) coincide that the most favorable experimental configuration to obtain transport parameters in these materials is the heat transmission configuration, in which the PA signal is detected at the rear side of the sample, opposite to its illuminated surface. A very useful arrangement is the so-called Open PA Cell (OPC) setup [20], that we will also describe later.

The scope of this paper will be as follows. In the next section we shall give a brief outline about the history of the investigations concerning the PA and PT effects in semiconductors. Then, in Section 3, we will present the

general theory of the photoacoustic signal generation in bulk materials before reviewing in 4 some works concerning the characterization of structures consisting by a film on a substrate for different configurations. In Section 5 we will describe how the photoacoustic technique can be used to measure the wavelength dependence of the optical absorption coefficient of semiconductor thin films. Section 6 will be devoted to briefly revise the state of the art of applications of photoacoustics for the characterization of porous semiconductor materials, in particular porous Si layers. Finally in 7 we will draw our conclusions.

2. Historical overview

To the best of the authors knowledge the first description of the PT effect in semiconductors dates from 1961, approximately two decades before the first developments in the fields of PT science and techniques appeared, when Gärtner [21] calculated the temperature distribution in an infinite slab in the case of small injection taking into account the nature of the incident optical radiation, the characteristics of optical absorption, the bulk and surface recombination mechanisms and the thermal properties of the material. Gärtner's model remained unknown for the photothermal community probably because it was developed for continuous illumination, whereas PA and PT techniques are based in time varying (pulsed or periodical) excitation.

The first attempt to give a quantitative investigation of non radiative processes involving electron transitions in solids using a PT technique (namely the PA one) is due to Murphy and Aamodt [22], who performed spectroscopic measurements of such processes in the luminescent laser material ruby ($Al_{2x}Cr_xO_3$) evaluating the influence of the Cr ions concentration, x. Quimby and Yen [23] have succeeded in measuring the ruby fluorescence quantum efficiency by developing a model which takes into account, for the first time, the rate equation and the life time for the metastable energy level to calculate the modulation frequency dependence of the photoacoustic signal to which the experimental data were then compared. The same authors [24] extended later the standard Rosencwaig-Gersho (RG) model [3] taking into account the possibility of spatial energy migration, i.e., they have accounted for the first time to the heat sources due to surface and bulk carrier desexcitation. These models for the PA signal generation taking into account the behavior of carriers under intensity modulated periodical excitation, established the basis for future research works in the field of semiconductors, where the first model considering the generation of free electrons and holes by light absorption, their diffusion and bulk recombination was developed by Miranda [25]. Approximately at the same

time Bandeira *et al* [26] developed the theory of the PA effect in an homogeneous semiconductor in a presence of an electrical field, which has been applied in order to enhance the PA effect from samples with low optical absorption coefficients via Joule heating, and Sablikov and Sandomirskii have also calculated the PA signal taking also into account the finite surface recombination velocity for semi-infinite [27] and finite [28] homogeneous semiconductors. The Sablikov and Sandomirskii theory was reviewed later by Gulyaev [29], who succeed in comparing some of their results with those of earlier experimental works of Mikoshiba *et al* [30], Jenkings [31] and Derch and Amer [32] using different PT approaches. These pioneering theoretical works show that the PT and PA effects in semiconductors can be used not only for obtaining information about the optical absorption coefficient (demonstrated in the early works of Rosencwaig [2]) or about thermal properties [33], but also as an alternative tool for measuring carrier recombination parameters. They have also stimulated further studies in this area. The possibilities of the PA technique for the measurement of recombination parameters was confirmed experimentally for the first time by Pinto-Neto *et al* in the bulk semiconductors PbTe, Si and GaAs [34, 35] via a heat transmission configuration that uses the air gas chamber adjacent to the membrane of an electret microphone as the photoacoustic gas chamber [20]. Further works using the same experimental methodology and almost similar theoretical models were reported in subsequent years [36-40]. The explicitly distinction between non-radiative (τ_{nr}) and radiative (τ_r) carrier lifetimes (more important when dealing with direct band gap semiconductors) was made for the first time by Marin *et al* [41] and their results were applied for the measurement of τ_{nr} in the “classical” III-V semiconductors GaAs, GaSb and InSb [41] and to the study of surface effects due to doping [42] and pasivation [43, 44], some of which will be reviewed later in this work. The mentioned works have only considered the influence of carrier recombination effects on the thermodiffusion (TD) mechanism [3] for the PA signal generation ignoring thermal expansion and thermoelastic (TE) sample bending, effects that can influence the signal at higher modulation frequencies. Sablikov [45] described the PT displacement of a semiconductor surface considering the deformation potential mechanism as the most important effect showing results that agree well with those obtained experimentally by Dersch and Amer [32]. The electronic deformation mechanism was included in the calculation of the PA signal in semiconductors by Stearns and Kino [46], and Todorovic *et al* [47-49] described the basic set of equations allowing the calculation of the influence of the TE and electronic strain (ES) mechanisms on the total PA signal. Solving their equations numerically they fitted the results of their measurements. With the aim of

explain an anomalous effect observed in photoacoustic experiments performed in Si samples Marín *et al* [50] developed a theory and have given an analytical expression, where the influence of carrier generation and recombination on the TD, TE, and ES mechanisms was taken into account. It is worth to mention that a similar result in Si samples coated with a carbon black layer was observed previously by Flaisher and Cahen [51], who attributed the effect to thermally induced surface deformations. The role of free carriers and interband absorption in the photogeneration of acoustic waves was also analyzed by Gusev [52, 53]. On the other hand, a theoretical framework for the interpretation of an important class of experiments performed in non-homogeneous semiconductors has been developed by several authors, which consider p-n [54-57] and metal-semiconductor junctions [58-59].

While the above mentioned works describe the theoretical basis for the understanding of frequency domain PT experiments in semiconductors, as well as for the interpretation of the results of spectroscopic PT measurements in these materials, we do not want to let mention to the so called PT microscopy experiments in semiconductor materials and devices, which have been developed after the early work of Rosencwaig [60]. Some of them are described in detail elsewhere [5]. Energy conversion processes and measurement of quantum efficiency in running semiconductor devices such as solar cells have been also investigated in the past by PT methods [61-64].

It is worth to remember, before finalizing this section, the coincidence that the ancient history of photoacoustics has also to do with semiconductors: Bell discovered the effect in the 1880s [65], when he developed a photophone [66] by impinging modulated light onto a semiconductor material, the selenium based receiver of his telephone circuit.

3. Theoretical model for the generation of the PA signal in bulk materials

When a solid is illuminated, absorption of optical energy can takes place, followed by the generation and propagation of thermal energy. If the solid is put in contact with the gas chamber in a closed PA cell and the impinging radiation is periodically modulated, the induced temperature changes produce an acoustic signal in the cell. From this it is possible, in general, to obtain information about thermal and optical properties of materials. As we have mentioned in the preceding section, further information may also be obtained if the photoexcited solid is a semiconductor material. In this case it is possible to obtain electronic transport properties of the photoinjected carriers.

The injected free carrier population will also perturb elastic constants and introduce local strains in the sample.

In what follows we will describe briefly the underlying theory for the most common used measurement variant for transport properties determination in semiconductors, namely the open PA cell (OPC) configuration. As mentioned above, heat transmission detection configurations are much suitable for the analysis of carrier transport properties in semiconductors. For example, Todorovic and Nicolic [39] demonstrated this on the basis of both theoretical calculations and experiments. They have show that the amplitude frequency dependence in the transmission configuration has more informative changes than the corresponding amplitude for front detection, for which the resulting lineal curve in log-log coordinates show a constant slope. Similarly, these authors observed that the signal phase in front detection is practically constant except for very low frequencies, thus carry out practically no information about the electronic transport properties of the sample. This behavior can be attributed to the high optical absorption at energies above the band gap, because the front detection signal depends mainly on the sample surface.

The OPC set-up can be realized by mounting the sample directly onto a circular electret microphone (Fig. 1), closing the (PA) air chamber in front of the electret diaphragm to get it hermetically sealed. The metallized electret diaphragm is connected through a resistor to a metal plate separated from it by an air gap. The periodical induced temperature variations and elastic vibrations in the sample, which follows the absorption of light energy, as well as the part of the incident radiation that can pass through the sample and reach directly the electret membrane [67], generate pressure oscillations in the PA chamber which deflect the membrane, generating a voltage across the resistor, which is often supplied to a FET pre-amplifier already built in the microphone capsule. Compared with other set-ups the OPC configuration has some advantages: The use of a minimal volume gas chamber allowing large PA signals is achieved using the front air chamber of the microphone as the transducer medium. The use of a common electret or condenser microphone (widely used in radio recorders) made this configuration cheaper than others. Likewise, the need to accommodate the sample in a closed conventional PA cell is not a limitation of the OPC and the loading, replacing and positioning of the sample is easier to perform. For the study of transport parameters, the photoacoustic signal phase and amplitude are measured using Lock-in synchronous detection as a function of the light beam modulation frequency at a given photon energy, while for optical absorption studies, i.e., PAS, the modulation frequency is fixed and the wavelength of the incident radiation is varied in the range of interest.

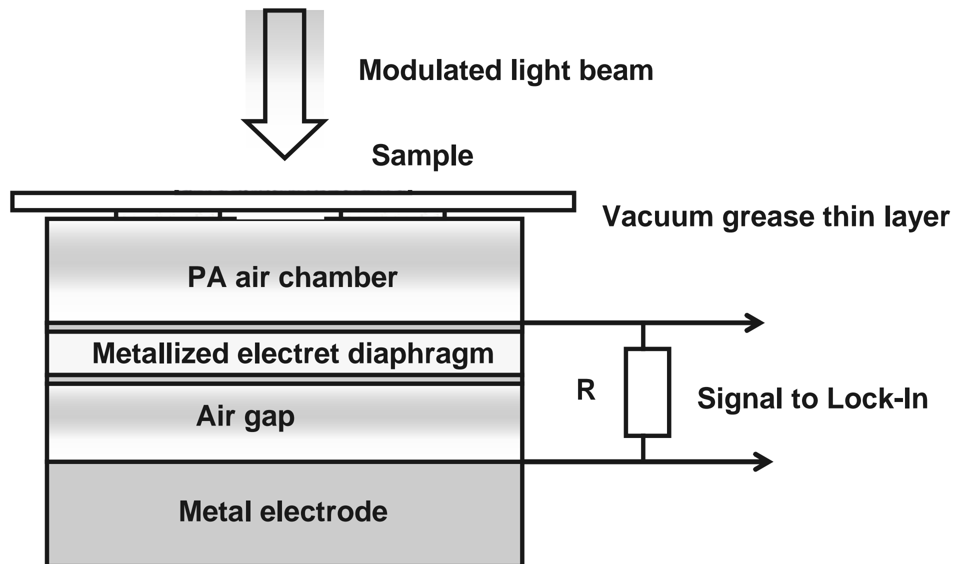

Figure 1. Schematic view of the Open Photoacoustic Cell configuration.

Consider the situation schematically depicted in Fig. 2. Modulated light of intensity I_0 impinges uniformly, in such a way that a one dimensional treatment will be valid, onto the sample of thickness L, an ideal semiconductor material with an optical reflection coefficient R and an absorption coefficient β at the incident photons energy E. The band gap energy will be denoted as E_g. One can demonstrate that the voltage given by the microphone, the so-called OPC signal, is related to the pressure fluctuation in the PA gas chamber, P(t), by means of:

$$V(t) = V_0 \cdot \frac{i \cdot \omega \cdot \tau}{1 + i \cdot \omega \cdot \tau} \cdot \frac{P(t)}{\gamma \cdot P_0} \tag{1}$$

where $\omega = 2\pi f$, f is the excitation light modulation frequency, τ is the microphone time constant, γ is the specific heats at constant pressure to constant volume ratio for air, P_0 is the ambient pressure and V_0 is a frequency independent constant. According to the composite piston model of Mc Donald and Wetsel [68] the pressure P(t) is the sum of various components:

First, when $E<E_g$ the semiconductor sample becomes transparent to the incident radiation, which impinges directly onto the membrane of the microphone thus generating a surface heat source leading to a pressure component P_m originated by thermodiffusion (TD) in the way described by the well known RG model [3]. According to this theory the generated heat diffuses into the gas layer in contact with the membrane surface, which expands and contracts periodically following the light modulation frequency

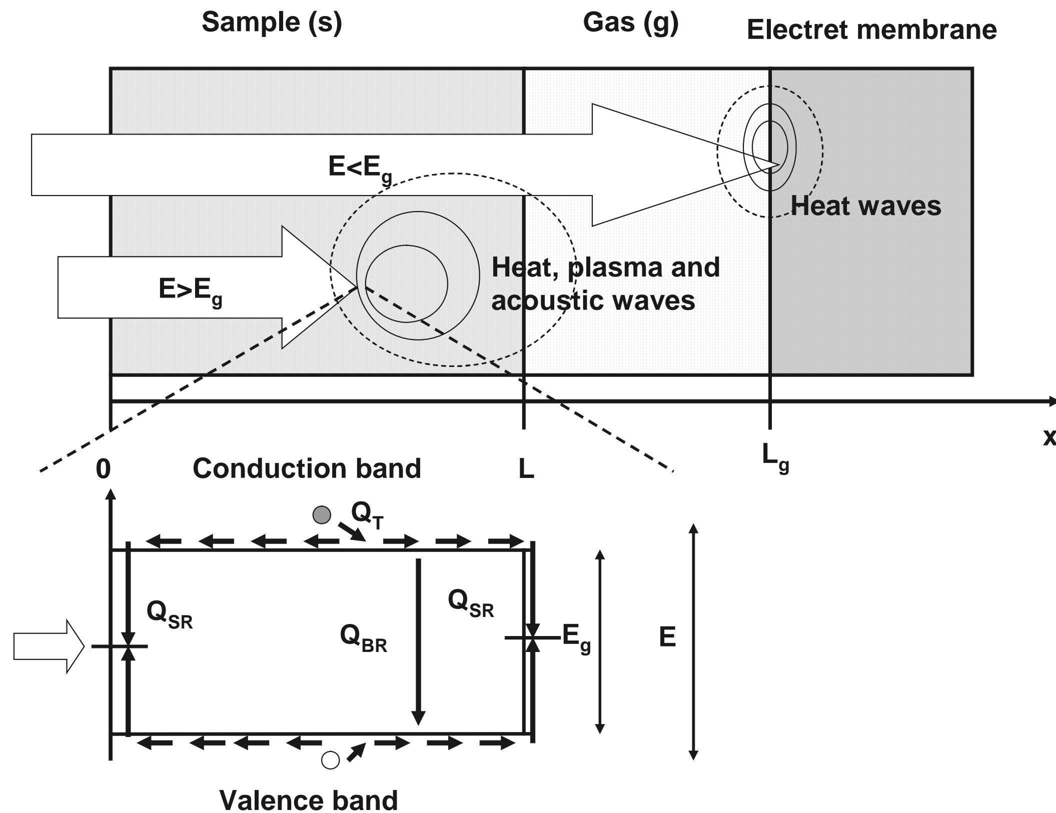

Figure 2. Schematic view of the different contributions to the PA signal in the OPC configuration.

and acting as a piston on the rest of the gas column inside the PA chamber thus generating acoustic waves.

The other sources contributing to the PA signal will be generated by photons of energy $E \geq E_g$, for which the sample becomes optically opaque. At a given distance from the sample's surface, determined by the inverse of its β value, a fraction of the incident radiation locally absorbed is converted into heat by the following processes: The first contribution to the pressure fluctuation, P_{TD}, is due to the thermodiffusion (TD) mechanism, similar as that explained above. The second mechanism is due to the thermoelastic (TE) bending mechanism described by the uncoupled set of TE and hydrodynamic (HD) equations [69, 20]. This effect is essentially due to the temperature gradient inside the sample along the axis perpendicular to the sample's surface of the Fig. 1 (namely the x axis shown in Fig. 2). The sample's displacement along the radial direction induces a bending of the sample in the x direction and as a consequence the vibrating sample acts as a mechanical piston which contributes to the signal with a component P_{TD} dependent on the value of the thermal expansion coefficient of the sample. Finally, a localized photogenerated carrier distribution confined within a thin layer beneath the

sample's surface introduces a local strain which, in turn, produces acoustic waves in the way similar as the local periodic thermal expansion does, which act as a piston onto the rest of the sample, thereby contributing to the signal. This mechanism was described by the first time by Figielski [70] and later observed in PA experiments by Stearns and Kino [46], Todorovic *et al* [47-49] and Marín *et al* [50]. It is denoted as the electronic strain (ES) mechanism and leads to a pressure contribution P_{ES}. It is directly related to the pressure dependence of the semiconductor band gap [70].

These three components can be calculated as described elsewhere [50]. They are directly related to sample and gas temperatures, which can be obtained solving the set of heat diffusion equations for the sample and PA chamber gas region with the properly boundary conditions [50] and taking into account the following heat sources (Fig. 2) [41]:

When the energy of the incident photons is greater than the band gap, its absorption will generate an excess of electron- holes pairs (EHP) with the same energy than the incident light, which, after a very short time ($\tau_{rel} \approx 10^{-12}$ s), thermalize giving up to the lattice the excess of energy E-E_g. This constitutes a fast heat source often called the thermalization heat source. It can be described by:

$$Q_t = \frac{(E - E_g)}{2E} \beta (1 - R) I_0 \tag{2}$$

After thermalization and during their lifetime part of the excess carriers diffuse away from the surface a distance inside the sample in average equal to their diffusion length L_n. After this process they recombine in the bulk of the semiconductor in a radiative or a non-radiative way. Only the later recombination mechanism will contributes to the PA signal. This is the non-radiative (nr) bulk recombination (BR) heat source characterized by the non-radiative carrier life time τ_{nr}:

$$Q_{BR} = \frac{E_g}{\tau_{nr}} \delta n \tag{3}$$

The parameter $\delta n(x,t)$ denotes the minority excess carrier concentration. The other carrier fraction can diffuses toward the front and rear sample's surfaces and recombine there non-radiatively through surface recombination centers leading to the non-radiative surface recombination (SR) heat sources characterized by the so-called surface (front and back) recombination velocities, S. The general expression describing this source is:

$$Q_{SR} = SE_g \delta n \tag{4}$$

Note that in both bulk and surface recombination, energy equal to E_g is converted into heat.

The excess carrier density is obtained from the carrier continuity equation:

$$\frac{\partial \delta n}{\partial t} = D_n \frac{\partial^2 \delta n}{\partial x^2} - \frac{\delta n}{\tau_T} + \frac{I_0 \beta (1-R)}{2E} \exp(-\beta x) \exp(i\omega t) \tag{5}$$

Here τ_T represents the overall carrier recombination lifetime and $D_n = Ln^2/\tau_T$ is the carrier diffusion coefficient in the material. Note that

$$\tau_T = \frac{\tau_r \tau_{nr}}{\tau_r + \tau_{nr}} \tag{6}$$

where τ_r is the radiative carrier recombination life time. The total carrier lifetime depends on the contribution of several recombination processes. For indirect band gap semiconductors the radiative recombination is very weak, since the conduction and valence band minimum does not lie at the same point of the Brilloin Zone and a third particle, i.e. a phonon, is required for radiative recombination. In the case of direct band gap semiconductors the radiative recombination is so efficient that the total carrier life time coincides in several cases with the radiative-one. This is the cause that in earlier works authors does not distinguish explicitly between non-radiative and total carrier life time in the heat sources given by Eq. (3). It is worth also to notice that in the most used models the authors does not considered the non linear dependence that can exists between the carrier recombination lifetimes and the concentration of the minority photoexited carriers in a semiconductor wafer. This is a very complicated problem leading to non analytical solutions. As the independence of carrier life time on the excess carrier concentration is valid for low generation rates care must be taken to work with small enough excitation light intensities so that this condition can be fulfilled.

One can demonstrate that the TE and ES components are, in general, important for high modulation frequencies, although the effect of the later has been proposed in the past as the cause of a so-called anomalous effect at relative low frequencies (see Ref. [50] for a discussion). Neglecting these components for which the corresponding expressions can be found elsewhere [50] and supposing that the sample length is much greater than the carrier

diffusion length so that back surface recombination can be ignored, Marín *et al* [41, 50] have obtained the following solution for the total pressure in the PA gas chamber that appears in Eq. (1):

$$P = P_{TD} = \frac{\gamma P_0 \left\{ \Phi_T + \Phi_{SR} + \Phi_{BR} \left[\left(\cosh(q_s L) + \frac{q_s}{q_p} \sinh(q_s L) \right) \exp(-q_p L) - 1 \right] \right\}}{L_g T_0 k_s q_g q_s \sinh(q_s l_s)} \quad (7)$$

where

$$\Phi_T = \frac{E - E_g}{2E} I_0 (1 - R) \quad (8)$$

$$\Phi_{SR} = \frac{E_g I_0 \beta (1 - R) S(D_p \beta + S)}{2ED_p (\beta^2 - q_p^2)(D_p q_p + S)} \quad (9)$$

$$\Phi_{BR} = \frac{q_p}{S\tau_{nr} (q_p^2 - q_s^2)} \Phi_{SR} \quad (10)$$

In the above equations T_0 is the ambient temperature, L_g is the PA chamber length, $q_j=(1+i)(\omega/2\alpha)$ (j=g, s) is the thermal wave number, $q_p=(1/L_n)(1+i\omega\tau_T)^{1/2}$ is the inverse of the complex carrier diffusion length, or plasma wave number, k and α represent thermal conductivity and diffusivity respectively, and the subindices g and s refers to the gas chamber and sample regions respectively.

Several works have been published using the OPC technique for the study of electronic transport properties of bulk semiconductors. In general it is difficult to determine a priori whether the thermal or electronic contribution is predominant in the measurement frequency region. Nevertheless, it is possible to identify the corresponding frequency regions using PA amplitude data. This procedure is essentially based upon recording of the OPC amplitude signal as a function of the modulation frequency. The PA amplitude signal exhibit changes in slope depending on the mechanisms causing it, because each term of Eqs. (8) to (10) have different frequency dependences. Identification of the frequency regions corresponding to each term and data fitting restrained to the these ranges can provides the values of τ_{nr} and S. Using this technique Pinto-Neto *et al* [34, 35] studied GaAs, PbTe and Si and Delgadillo *et al* [71] performed the characterization of CdTe samples.

Other authors have calculated the PA signal in the total frequency range where the experiment was performed [41-44]. Fig. 3 shows the result of numerical simulations using Eq. (1) for a typical GaAs sample from which one can see how changes in the recombination characteristic parameters affects strongly the phase of the PA signal voltage. The parameters used for the calculations were taken from Ref. [41]. The existence of minimums in the signal phase, whose positions can change with variations in *S* and τ_{nr} should be helpful for the fitting procedure. Part (a) of the figure shows the influence on the phase of variations in the carrier non radiative recombination lifetime for a fixed surface recombination velocity while in part (b) we have represented how the phase is influenced by changes in the later parameter.

Using the above model the recombination lifetimes for bulk samples of n-GaAs (10^{18} cm^{-3}), p-GaSb (2×10^{16}) and n-InSb (10^{16}) were measured by Marín *et al* [41]. The values $(7.5\pm0.1)\times10^{-7}$s, $(9.1\pm0.4)\times10^{-7}$s and $(3.82\pm0.03)\times10^{-7}$s were obtained respectively. These times were attributed mainly to band to band Auger recombination processes although the technique does not distinguish between the actual recombination mechanisms. Nevertheless, taking into account that reported data of these times are subject to considerable uncertainties the agreement between experimental measured and reported values was quite satisfactory.

Passivation studies have been also performed in the past using the above described methodology. Riech *et al* [43] demonstrated that a strong dependence of the surface recombination velocity at the SiN/Si interface on the silane to ammonia ratio used for the growth of SiN films on Si using the

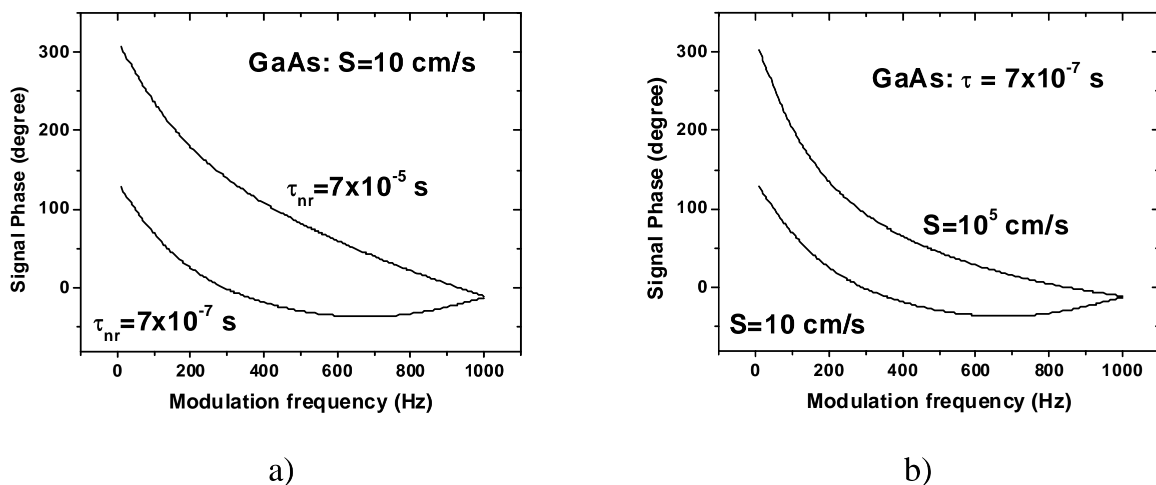

Figure 3. Numerical simulations of the phase of the PA signal voltage given by Eq. (1) as a function of the modulation frequency for a typical GaAs sample. a) Influence of τ_{nr} on the phase for a fixed *S*. b) Influence of *S* on the phase for a fixed τ_{nr}. Parameters for calculations were taken from Ref. [41].

PECVD (Plasma Enhanced Chemical Vapor Deposition) technique. Their results were correlated (Fig. 4) with those obtained for the midgap surface state density determined by Capacitance-Voltage (C-V) measurements in Metal-Insulator structures (MIS) fabricated in similar Si wafers. In this way the mentioned authors showed that the PA technique may be used as a valuable tool for the estimation of the surface recombination velocity since it is a simple and non-invasive technique.

It is worth to mention that since the first reported theoretical works several groups have tried to improve the theory of PA signal generation in semiconductors, but all quintessentially possessed the same foundations as the here presented. Note that if $\Phi_{SR}=\Phi_{BR}=0$ and $E_g<<E$ (as in a metal) the solution of the above described problem is similar to the well known result from the RG theory [3]. Covering the semiconductor surface facing the light beam with an opaque metal film eliminates the carrier contributions to the signal since the light energy is no longer absorbed by the sample. If the metal is thermally thin it will acts as an instantaneous heat source at the sample's surface. The signal will no longer depend on carrier transport parameters and it will be given by the RG theory. From its modulation frequency dependence thermal diffusivity can be obtained as reported elsewhere [72].

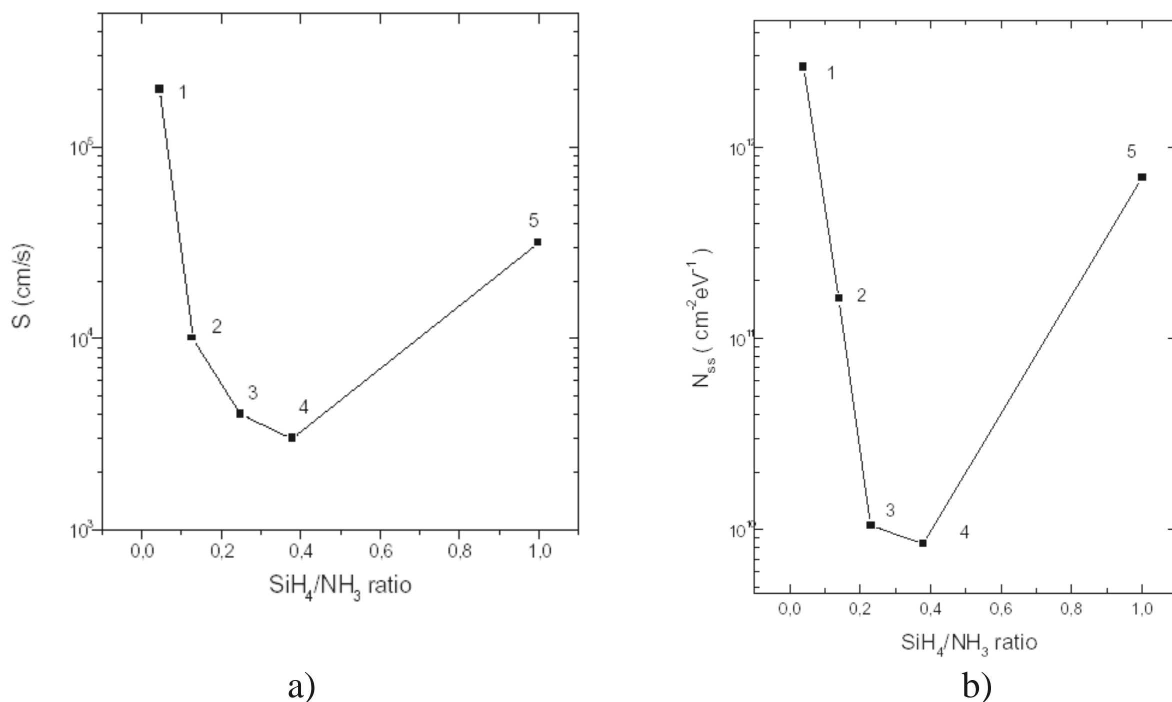

Figure 4. Behavior of the surface recombination velocity determined by PA (a) and the mid gap surface state density measured by C-V (b) with the silane to ammonia ratio used for the growth of SiN films on Si by PECVD. (Reproduced from Ref. [43] with permission of Institute of Physics, IOP).

4. Measurement of electronic transport properties of two layer systems. The case of a semiconductor layer on a semiconductor substrate

It is very common in micro- and optoelectronic that semiconductor materials be deposited on substrates. These structures can be formed by a semiconductor material grown as a thin film on the substrate, by oxide coating or metal deposition on its surface, among others. While an example of the influence of a dielectric isolating layer on the semiconductor electronic surface properties was discussed in the foregoing section, in this paragraph we will focus our attention to the semiconductor-semiconductor case, showing results obtained using the OPC configuration for different kinds of structures regarding the nature of the energy band gaps of the involved materials, as well as the direction of incidence and energy of the excitation light. We will analyze only particular cases, in which the band gap energies of the film and the substrate have different values, i.e., we do not will discuss here the case of p-n junctions formed within the same material. Two systems will be discussed: a wide band gap layer on a narrow band gap substrate and the inverse structure, the case of a narrow band gap layer/wide band gap substrate. The excitation energy will be in all cases greater than the band gap of both semiconductors and we will suppose that the excitation light impinges on the layer side, while the substrate faces the electret microphone.

As we will seen, the theoretical description of the PA effect for a two layer system is very similar to the description of one-layer semiconductor given in the previous section, with the particularity that the heat sources existing in each layer should be taken into account. This makes very difficult to get analytical solutions of the corresponding set of heat diffusion equations and boundary conditions, therefore in many cases the problem is solved numerically.

4.1. Wide band gap layer/ narrow band gap substrate

Let us consider the geometry represented in Fig. 5, showing a semiconductor layer (region 1) with energy gap E_{g1} and a substrate (2) with energy gap E_{g2} ($E_{g1} > E_{g2}$) in contact with the PA chamber (g). The absorbed photons of energy E, which is greater than both band gap energies (note that otherwise, i.e. if $E<E_{g1}$ and $E>E_{g2}$, one becomes a situation similar as that described above for the system SiN/Si), create in the layer an excess carrier concentration δ_{n1}. These photoexcited carriers thermalize and diffuse through the film after they recombine in its bulk and its surface at x=0 creating the heat

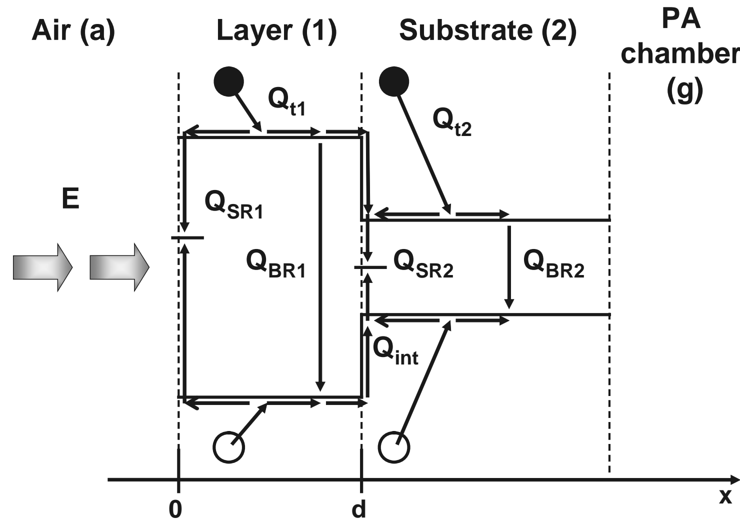

Figure 5. Heat sources in a wide band gap/narrow band gap semiconductor structure.

sources Q_{t1}, Q_{BR1} and Q_{SR1} similar to those described by Eqs. (2), (3) and (4) respectively, but with values of the involved parameters corresponding to the layer material. If the layer thickness d is lower than the optical diffusion length in the material, then the laser beam energy is not completely absorbed in the thin layer and will generate photoexcited carriers in the substrate too, which thermalize to the band extreme and diffuse to the layer-substrate interface and to the bulk of the substrate creating the corresponding heat sources there. The thermalization and bulk recombination terms are given also by expressions similar to Eq. (2) and (4) respectively (with the parameters corresponding to the substrate material).

Photogenerated minority carriers which have reached the interface by diffusion from the layer, will thermalize to the band extreme of the substrate creating phonons, and hence, heating the interface plane. This thermal source Q_{int} can be written as:

$$Q_{\text{int}} = \left(E_{g1} - E_{g2}\right)\delta n_1\left(d\right)\frac{l}{\tau_{rel}} \tag{11}$$

where l is the carrier mean free path and τ_{rel} is the relaxation time of the carriers when they go from the band extrema in the layer to those in the substrate material. Finally, carriers that came by diffusion from the layer and from the substrate may also recombine at the substrate/layer interface, generating a heat source of the form

$$Q_{SR2} = E_{g2}S_2\delta n\left(d\right) \tag{12}$$

where S_2 represents the interface recombination velocity.

In the above equations $\delta n = \delta n_1 + \delta n_2$, where δn_1 and δn_2 are determined from the solution of the carrier diffusion equations with appropriate boundary conditions in the layer and in the substrate respectively.
Then the system of equations to be solved becomes:

$$\begin{aligned}
&\frac{\partial^2 \Theta_a(x)}{\partial^2 x} - q_a^{\ 2}\Theta_a(x) = 0\\
&\frac{\partial^2 \Theta_1(x)}{\partial^2 x} - q_1^{\ 2}\Theta_1(x) = -\frac{E_{g1}}{\tau_{nr1}k_1}\delta n(x)\\
&\frac{\partial^2 \Theta_2(x)}{\partial^2 x} - q_2^{\ 2}\Theta_2(x) = -\frac{E_{g2}}{\tau_{nr2}k_2}\delta n_2(x)\\
&\frac{\partial^2 \Theta_g(x)}{\partial^2 x} - q_g^{\ 2}\Theta_g(x) = 0
\end{aligned} \tag{13}$$

With the following boundary conditions:

$$\begin{aligned}
&\Theta_a(0) = \Theta_1(0)\\
&-\frac{k_a \partial\Theta_a(0)}{\partial x} = -\frac{k_1 \partial\Theta_1(0)}{\partial x} + S_1 E_{g1}\delta n_1(0) + \frac{h\nu - E_{g1}}{\beta_1}G_1(0)\\
&\Theta_1(d) = \Theta_2(d)\\
&-\frac{k_1 \partial\Theta_1(d)}{\partial x} = -\frac{k_2 \partial\Theta_2(d)}{\partial x} + S_2 E_{g2}\delta n_2(d) + \frac{h\nu - E_{g2}}{\beta_2}G_2(d) + \frac{E_{g1} - E_{g2}}{\tau_{rel}}\delta n_2(d) l_{rel}\\
&\Theta_2(d1) = \Theta_g(d1)\\
&-\frac{k_2 \partial\Theta_2(d1)}{\partial x} = -\frac{k_g \partial\Theta_g(d1)}{\partial x}
\end{aligned} \tag{14}$$

In the above equations Θ_j represent the spatial part of the temperature distribution in the j-th region (j=a, 1, 2, g), k_j is the thermal conductivity, $q_j=(1+i)(\pi f/\alpha_j)^{1/2}$ is the thermal wave number, with α_j as the thermal diffusivity, G_j represents the generation rates (see later) and S_1 is the surface recombination velocity at x=0. The variables τ_{nr1} and τ_{nr2} are the non-radiative recombination carrier lifetimes in the regions 1 and 2 respectively. The carrier concentrations δn_j should be obtained from the system of carrier diffusion equations for the j-th regions that can be written as:

$$D_j \frac{\partial^2 \delta n_j}{\partial x^2} - \frac{\delta n_j}{\tau_{Tj}} + G_I = 0 \quad j = 1,2 \tag{15}$$

where τ_{Tj} and D_j are the total carrier recombination time and the carrier diffusion coefficient of region j respectively, with the boundary conditions:

$$
\begin{aligned}
& D_1 \left.\frac{\partial \delta n_1}{\partial x}\right|_{x=0} = S_1 \delta n_1 (x=0) \\
& D_2 \left.\frac{\partial \delta n_2}{\partial x}\right|_{x=d} = S_2 \delta n_2 (x=d) - \frac{J_n(d)}{q} \\
& \delta n_2 (x \to \infty) \to 0
\end{aligned}
\tag{16}
$$

where J_n represents the current density and q is the electron charge.

In the above equations the generation rates can be written as:

$$
G_j = \begin{cases} I_0 (1 - R_j) \beta_j \exp[-(\beta_j x)] & j = 1 \\ I_0 (1 - R_{j-1})(1 - R_j) \beta_j \exp[-(\beta_{j-1} x)] \exp[\beta_j (x - d)] & j = 2 \end{cases}
\tag{17}
$$

with β_j and R_j as the optical absorption and reflection coefficients respectively of region j at the photons energy.

Solving Eqs. (13) to (17) one can calculate the PA signal in the layer/substrate semiconductor structure for a particular system.

Riech *et al* [44] studied the influence of the Al content, x, (x=0.3 and x=0.7) of an $Al_xGa_{1-x}As$ layer of thickness d=0.1μm grown on a GaAs substrate by liquid phase epitaxy (LPE), on the electronic quality of the layer/substrate interface. GaAs is a well known semiconductor material with applications mainly in optoelectronic light emitting devices such as LEDs and Lasers and in high speed microelectronic. Nevertheless, its electronic properties are governed by an undesirable high surface recombination velocity. One of the used methods to reduce S in the GaAs substrate surface is the growth of a thin $Al_xGa_{1-x}As$ layer with a low Al content over it. In the mentioned work the authors have shown the usefulness of the PA technique as an alternative to evaluate the GaAs surface quality by means of the measurement of S. They used a theoretical model described above, where symbols 1 and 2 referred to the AlGaAs layer and the GaAs substrate respectively. The calculated phase of the PA signal as a function of the light modulation frequency shows a minimum, which moves towards the lower frequencies as S_2 decrease. On the other hand the phase difference also decreases with S [44]. These features could help to comparative analysis between samples with similar characteristics and different values of the interface recombination velocity.

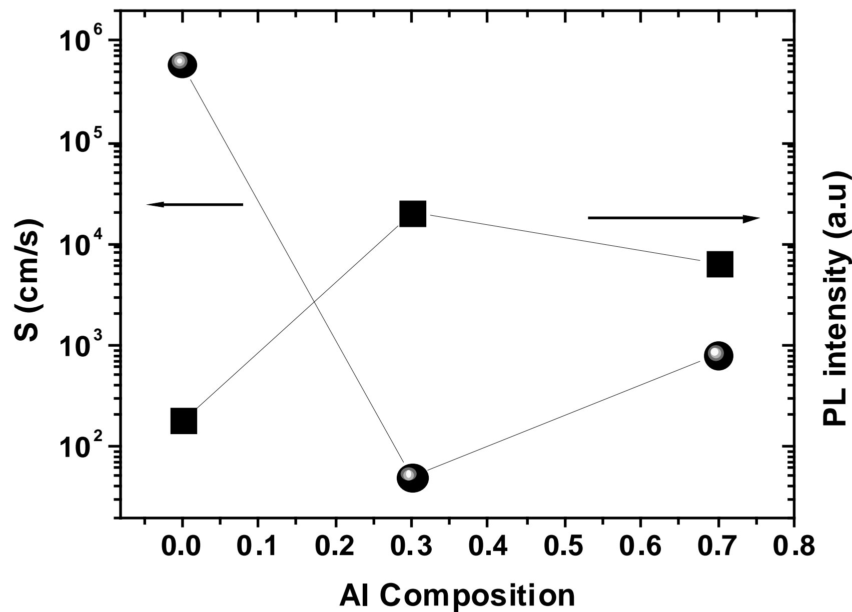

Figure 6. Measured recombination velocity as a function of Al content at the interface AlGaAs/GaAs with d=0.2 μm and photoluminescence intensity of the exciton line as a function of Al composition in the layer. The PL spectra have been excited at 80 K using a 10 mW HeNe laser of λ=620 nm (Reproduced with permission from [44] Copyright 1999, American Institute of Physics).

Experimental data taken using the OPC detection configuration and an Ar ion laser of wavelength λ=488nm as the light source are show in Fig. 6. By fitting the theoretical model to the experimental PA phase data, the interface recombination velocity was determined. This parameter is shown as the function of the Al content. For comparison we show the photoluminescence intensity of the 1.504 eV line, which is due to the exciton bound to the C acceptor, as a function of x.

The peak intensity decrease is due to the fact that more photoexcited carriers recombine at the interface, i.e., the PL intensity is an indirect measure of how the surface and hence the recombination velocity change.

4.2. Narrow band gap layer/ wide band gap substrate

This configuration is shown schematically in Fig. 7. Several particular situations can be analyzed. If we suppose, as in the above section, that the laser beam energy is greater than the band gap energy of both, layer and substrate, and that the layer thickness is lower than the optical penetration length, i.e. the layer is optically semitransparent, heat generation will take place in both layer and substrate, and the calculation of the PA signal will occurs in a way similar as described in the previous section.

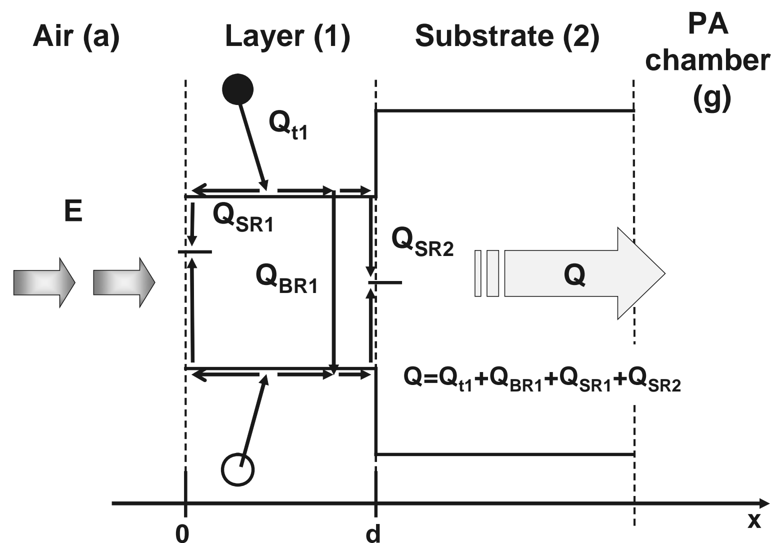

Figure 7. Schematic view of the heat sources present in the system narrow band gap / wide band gap semiconductor for a type I structure. The excitation energy E is greater than both layer and substrate band gaps and the layer is optically opaque at this energy.

When the layer is optically opaque the incident light is absorbed only within it. As a consequence three processes contribute to the PA signal, namely intraband thermalization, nonradiative bulk recombination and carrier recombination at both the sample surface and the layer-substrate interface. Each one of these mechanisms generates thermal sources Q_{t1} Q_{BR1}, Q_{SR1} and Q_{SR2} respectively, as shown in the figure 7. Note that the same occurs when the conditions $E>E_{g1}$ and $E<E_{g2}$ are fulfilled, independently of the layer thickness. Because the excitation light is totally absorbed in the thin film then no heat generation mechanism will be present in the substrate, therefore it will plays only the role of a thermal diffuser and only their thermal properties will contribute to the PA signal.

Following the above analysis one can construct the corresponding system of heat diffusion and continuity equations with the properly boundary conditions to find the dependence of the PA signal on the carrier transport parameters of the semiconductor layer in a way similar as we do in the previous section. Thus this straightforward procedure will be not discussed here.

While the system represented in Fig. 7 constitutes a Type I structure respecting the energy bands alignment, we can also have a Type II system. One typical example is the GaInAsSb/GaSb structure showed in Fig. 8, in which the valence band of the GaSb substrate lies above the valence band of the GaInAsSb layer. $Ga_xIn_{1-x}As_ySb_{1-y}$ alloys (x and y denotes here the Ga and

As volume concentration, respectively) have been extensively proved in the optoelectronic industry for the fabrication of photovoltaic devices, lasers and sensors, because they offer a spectral range that is suitable for optical fiber communications and environmental monitoring. However, applications are limited because non-radiative recombination through Auger processes in the quaternary alloy seriously affects the efficient performance of these devices. Riech *et al* [73] reported for the first time about the measurement of the recombination life time associated to these mechanisms in the GaInAsSb material, as we will describe below.

The PA signal generation mechanisms for this structure are represented schematically in Fig. 8. We suppose as above that the layer is optically opaque and that the photons energy is greater than both layer and substrate band gaps energies. Thus the excitation light is absorbed only in the GaInAsSb layer generating electron-hole pairs in the valence and conduction bands which thermalize to the band extrema, diffuse through the layer, and recombine in its volume and at both, its surface and its interface with the substrate.

As we can see the photoexcited minority electrons remain at the narrow gap semiconductor due to the conduction-band potential barrier at the interface, while the holes can ‘thermalize to the valence-band extreme of the GaSb substrate creating phonons and, hence, generating the thermal source Q_{int}. The holes that diffuse and recombine non-radiatively into the bulk of the substrate will create the thermal source Q_{B2}.

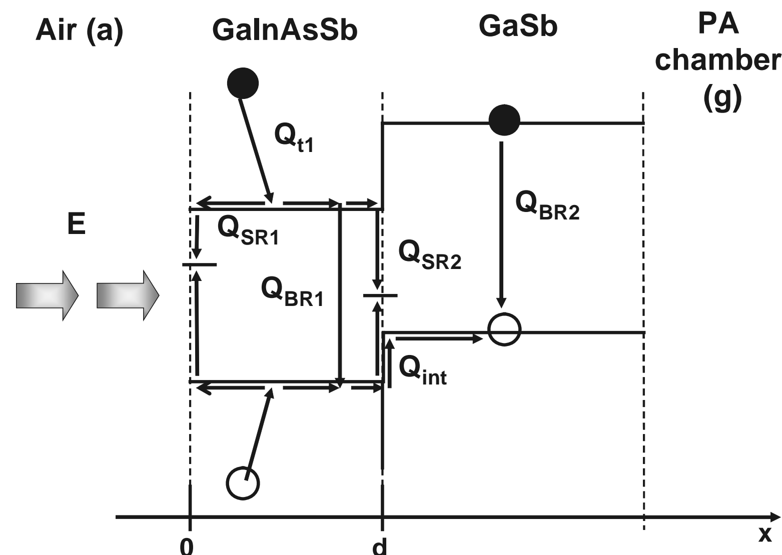

Figure 8. Schematic view of the heat sources present in the system narrow band gap / wide band gap semiconductor for a type II structure such as the GaInAsSb/GaSb discussed in text. The excitation energy E is greater than both GaInAsSb-layer and GaSb-substrate band gaps. The former is optically opaque at the photons energy.

In Fig.9a we show typical experimental curves corresponding to the PA phase signal as a function of the modulation frequency. The solid curves represent the best fit of the theoretical model developed taking into account the heat generation mechanisms showed in Fig. 8 (see Ref [73] for details). The non radiative (Auger) recombination time was left as the adjustable parameter. The values of the other parameters were taken from the literature or were calculated using interpolation formulas for the quaternary material. The value of $\tau_{AUGER}=(0.82\pm0.07)\times10^{-6}$s was obtained as a mean result of several measurements performed in different samples. Using this result the Auger recombination coefficient $C=1.22\times10^{-28}$ cm^6/s have been calculated, which inserts quite well in a recompilation of experimental and theoretical data reported in the literature for direct-bandgap III–V compounds, as shown in Fig. 9b [73].

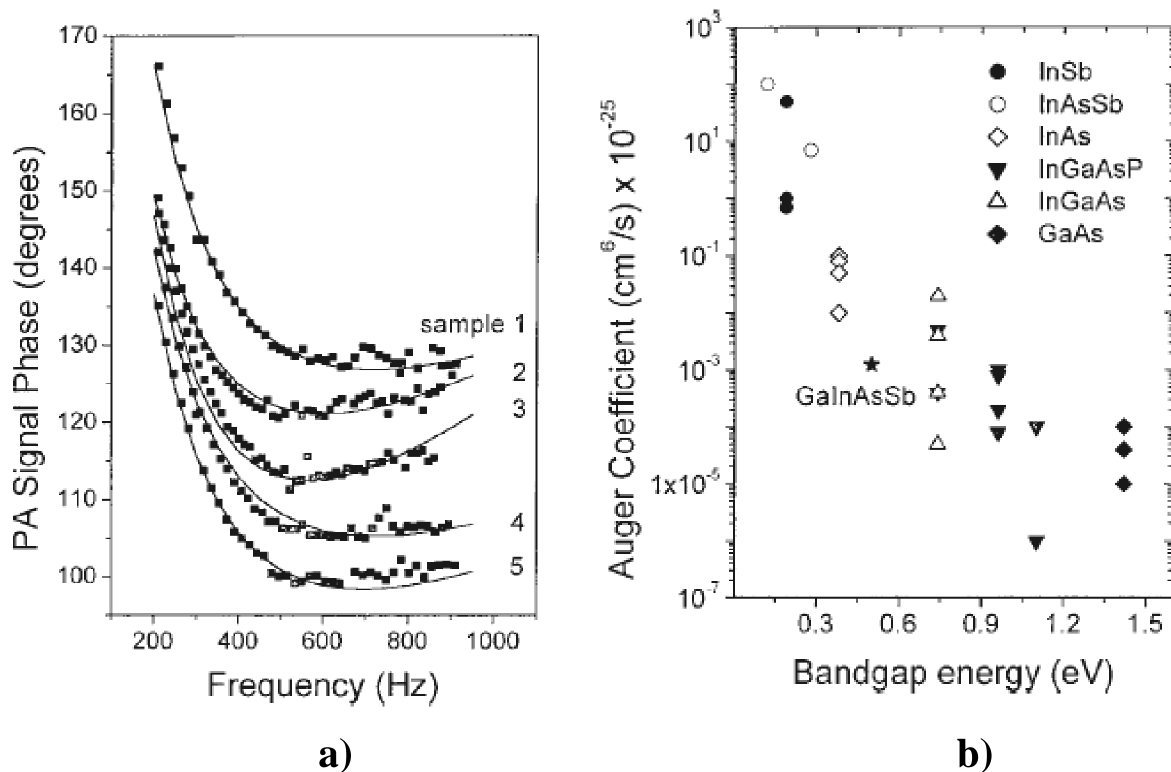

Figure 9. a) PA signal phase as a function of the modulation frequency for different $Ga_xIn_{1-x}As_ySb_{1-y}$ samples (sample 1: x=0.83, y=0.08, d=3μm; 2: x=0.83, y=0.09, d=5μm; 3: x=0.83, y=0.10, d=5μm; 4: x=0.82, y=0.13, d=4μm and 5: x=0.82, y=0.15, d=5μm). The quaternary material was grown on p-type (100) GaSb by LPE at 850^0C. The layers were also p type and were intentionally non-doped. Excitation was performed using a 180mWAr-ion laser (E=2.54 eV) b) The Auger recombination parameter for different III-V compounds showing the value obtained as described in the text for the GaInAsSb compound. (Reprinted with permission from [73] Copyright 2001, American Institute of Physics).

Before concluding this section we will refer to the important case of an insulator substrate. Thin films deposited on a glass substrate concern to this kind of structure which is very common in thin film solar cells and gas sensors, among others. The analysis of the generation of the PA signal is very similar to the case treated above in the sense that heat generation takes place only in the semiconductor layer. The greatest difficulties arise in connection with slightly absorbent samples in which special care should be taken to avoid absorption of the laser beam by the microphone electret membrane.

Early reports analyzing semiconductor thin film/transparent-substrate by the PA technique are due to the works of Todorovic *et al* [38], which studied thermal and transport properties of amorphous GeSe thin film deposited onto a quartz substrate. Experimental results show that the PA signal is strongly dependent on the sample position in the PA cell, i.e. if the optical excitation takes place on the side of layer or of the substrate. When the substrate is turned towards the light beam source and the thin film towards the PA cell the influence of the later on the signal becomes significant, while in the opposite configuration the thin film acts only as a surface heat source on top of the quartz substrate which becomes a media through which heat diffusion occurs influencing the PA signal. It is necessary therefore to take care to avoid damage of the thin film layer by the mechanical contact with the microphone or with the vacuum grease used often to seal the PA chamber. Thin film parameters such as ambipolar diffusion coefficient, surface recombination velocity and lifetime were calculated by fitting a theoretical model to the PA amplitude and phase data. It was concluded that due to the fact that the thin films are much thinner than the substrate, at low modulation frequencies the signal phase is mainly influenced by the film thermal properties, while at higher frequencies the electronic transport properties begin to play a significant role. Therefore, a two step fitting procedure was proposed: first the optical and thermal parameters were determined in a low frequency range and then, using these values, a fit in the higher frequency range was performed to find the transport parameters. Another example can be found in the works of Bernal-Alvarado *et al* [74] and González *et al* [75], which fitted the resulting expression for the signal phase for thermally thick and optically opaque samples to determine transport properties for the CdTe/glass system.

5. Photoacoustic spectroscopy in thin films

As mentioned above, the dependence of the PA signal on the absorption coefficient allows perform spectroscopy studies and therefore, since the first reported works (see Ref. [2]), PAS has been applied to the measurement of the absorption spectra of semiconductors materials. PAS measurements are

simple and can be performed on any kind of solid material. In fact, as Rosencwaig [2, 3] had demonstrated, in conventional PAS only the absorbed light produces an acoustic signal, while scattered light, which often presents a serious problem in conventional spectroscopy, can be very frequently neglected. Another advantage of PAS is the possibility of analyzing samples at different depths by variation of the light modulation frequency. For example, for a sample of Si, at 10 Hz and 300 Hz the thermal diffusion length of thermal waves are about 1700 and 300 μm respectively. This is a great distance in contrast with the penetration depth of the incident optical photons (supposes they have energy approximately equal to 1.3 eV, then their penetration depth is about 100 μm). Therefore, with PAS we can obtain information from regions not conventionally accessible by optical techniques. Thus one could also envisage probing non heterogeneous samples, such as the two layer systems that, as we have mentioned in the previous section, are often encounter in praxis. Both the amplitude and the signal phase can be considered proportional to the optical absorption coefficient but, because they depend on the physical and geometrical characteristics of the experimental apparatus, the determination of the value of this parameter from the amplitude and phase spectra is quite complex, although some authors [76] have reported about the possibility of its determination from the simultaneously analysis of the two measurement channels. Inspired in a previous work of Christofides *et al* [77], which have reported on similar measurements in bulk crystalline Ge samples using photopyroelectric detection, Vigil *et al* [78] have demonstrated recently the possibility of β determination by PAS in thin films grown on transparent substrates using the OPC transmission configuration of Fig. 1. As we have mentioned in the introduction the knowledge of the wavelength dependence of the optical absorption coefficient is very important in thin films, but very opaque materials are difficult to be characterized by other techniques. OPC-PAS measurements were demonstrated in the past by Marquezini *et al* [67] for the measurement of the absorption spectra of green leaves. In what follows we will present some recent developments in the field of semiconductor thin films optical characterization.

Consider the OPC configuration described above (Fig. 1) and a sample constituted by a thin film on a transparent glass substrate, which closes the (PA) chamber with the substrate facing the microphone to avoid damaging the thin film by mechanical contact. The light provided by a high intensity lamp is modulated at a fixed frequency with a mechanical chopper after it passes through a high resolution monochromator in order to obtain monochromatic light in the spectral range of interest. The light is then focused onto the thin film side of the sample. A glance at Fig. 1 shows that in

the spectral region near and bellow the energy band gap, where the film becomes transparent, the transmitted modulated light impinges directly on the metallized electret diaphragm, where it is absorbed generating pressure fluctuations in the PA chamber as described before. The signal is then proportional to the sample's optical transmittance. On the other hand, when the semiconductor absorbs photons with energies above its absorption edge it will be appreciated that electron excitations, having a finite lifetime, are generated, accompanied by the generation of electron-hole pairs, which also exist for a finite lifetime and move within the sample, before transferring their energy back to the sample in the form of heat by the processes described in the preceding sections, thus inducing pressure oscillations in the PA air chamber. Taking these mechanisms into account, and in order to eliminate the glass substrate and electret diaphragm contributions, the PA absorption spectrum was recorded by dividing, for each photons energy value, the signal due to the sample/glass system, V_s, by that due to the direct incidence of the modulated light on the diaphragm after passing through a glass substrate placing instead the sample, V_i (in this last configuration the PAS spectrum will reproduce the emission spectra of the lamp). For thermally thick samples the absorption coefficient is then calculated as described elsewhere [78].

The method has been applied to the study of the influence of Bi-doping on the optical absorption of CdTe thin films [78]. CdTe have been attracted much attention as promising material for photovoltaic energy conversion applications. CdTe thin films obtained by high-temperature processes such as CSVT (close space vapor transport) are typically fabricated with thicknesses ranging from 3 to 15 μm having absorption coefficients very difficult to determine optically. One of the physical properties that must be improved in solar cells is the electrical resistivity of the CdTe absorber film. In general, as-grown CdTe thin films show a high electrical resistivity, with a slight p-type conductivity due to stoichiometric defects (Cd vacancies) acting like acceptor centers. In order to decrease the resistivity, CdTe doping with elements like Sb [79] or Te [80] has been achieved. The possibility to obtain CdTe:Bi thin films with resistivity values lower than those corresponding to the undoped ones for Bi concentrations of about 1×10^{18} cm^{-3} have been demonstrated elsewhere [81]. CdTe thin films were deposited onto different substrates by CSVT using CdTe powders (99,99 % purity) and powders obtained from sintered CdTe:Bi monocrystals grown by the Bridgman technique. The substrates used in these experiments were soda-lime glasses.

Fig. 10 shows absorbance derivative versus photon energy plots as obtained from OPC-PAS measurements, which displays well-resolved structures composed of one band.

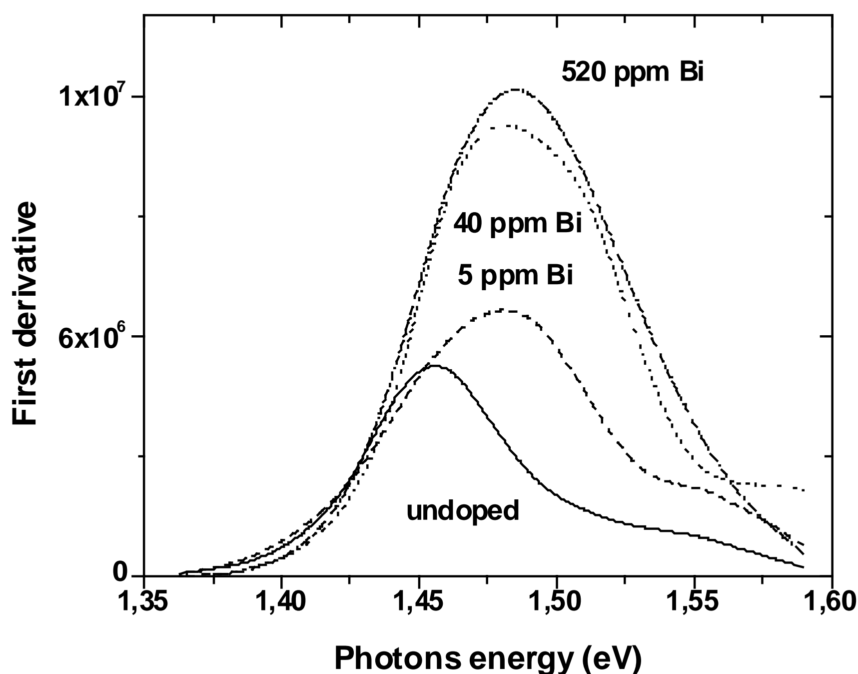

Figure 10. The first derivates of absorption spectra for undoped and Bi doped CdTe films deposited onto glass substrates: Undoped (solid); CdTe:Bi (5ppm) (dash); CdTe:Bi (40 ppm) (dot) and CdTe:Bi (520 ppm) (dash dot). (Reproduced with permission from Ref. [83]).

These curves allow us to calculate the exact value of the band–gap energy. Values of 1.46, 1.46 eV, 1.49 and 1.48 eV where obtained for the undoped and doping films at 5, 40 and 520 ppm respectively.

This apparent abnormal behavior has been attributed to the amphoteric behaviour of Bi in the CdTe host, as demonstrated also by Photoluminescence (PL) and electrical measurements [82]. While undoped samples are p-type with a high electrical resistivity, as common observed for this material, at low concentrations Bi atoms replace Cd vacancies introducing donor levels. For higher concentrations they replace Te vacancies, becoming acceptors, and the film becomes p-type again, but with a higher electrical resistivity than the value corresponding to the undoped material [82]. More details about these experiments are given elsewhere [83].

6. Porous Si

Last, but not least, we will refers us briefly to the important class of materials called porous semiconductors. Although porous structures of different semiconductor materials have been investigated as well [84], more emphasis have been made in porous Si (PS). Since Canham found in 1990 [85] that PS shows efficient luminescence at room temperature, a strong

interest have been developed on both the cause of the light emission mechanism and possible applications of this material in optical devices, but also in insulator structures, gas and biochemical sensors, and so on.

PS samples made by a porous layer over a crystalline substrate are usually produced by anodic etching of a crystalline silicon wafer in hydrofluoric solution [86], although spark erosion techniques have been also employed [87, 88].

For any application it is very important to study the optical, electronic and thermal properties of PS, especially it is desirable to measure the properties of the PS layer without separating it from the substrate. Although a lot of studies have been done on photoluminescence (PL) of the porous layers, the papers dealing with optical absorption [89] and measurement of transport properties are not too numerous, perhaps because it is difficult to perform certain measurements using conventional techniques without removing the layers from the substrate. In the case of optical absorption measurements the main difficulty arises from the diffuse light scattering in the PS layer that contributes significantly to the resulting light extinction. As mentioned in previous sections the PA technique have proved to be a powerful tool to the study the optical, electronic and thermal properties of samples in a noncontact and nondestructive manner, and without a particular sample preparation procedure which hardly applies to PS.

The first report on PAS characterization of PS dates from 1994, when Brodin *et al* [90] used the technique for absorption spectra measurement and for the determination of the effective thermal diffusivity of the system composed by the PS layer and the crystalline substrate. Using effective medium theories Calderón *et al* have obtained for the first time the thermal properties of the porous layer for both anodically etching [91] and spark obtained PS [92]. In the first case the columnar characteristic structure was modeled by means of the analogy between electrical and thermal phenomena considering the whole sample as a combination of a parallel system (the PS layer) in series connected with the Si substrate [91]. In the case of PS obtained by spark, the sponge like layer of PS was modeled using the well known Maxwell's model [93] for a disperse phase in a continuous matrix [92].

Respecting PAS measurements the main objective of the published works is the measurement of the absorption edge of PS and the study of how its position can be influenced by factors such as the growth parameters, the particle size [94], and aging, among others. The most authors [95, 96] have been used the conventional PAS scheme in which the sample is illuminated on the PS layer and the PA signal is detected on the same side. When experiments are performed at sufficient low frequencies so that the thermal diffusion length in PS becomes larger than the layer thickness, the PA signal

is produced by light absorption followed by heating of both the porous layer and the backing crystalline substrate. When higher frequencies are employed the PA signal is determined by the porous layer alone if the thermal diffusion length becomes of the same order of magnitude as the layer thickness. The PAS spectrum of PS measured by different authors reveal several spectral features which demonstrates the complicated energy structure of PS due to the band gap widening as a result of quantum confinement effect and differences attributed as coming from surface effects and peculiarities of the samples preparation method. [97]. In the same way that the certain origin of the luminescence is still unknown, there are several unsolved questions in the explanation of the observed PAS spectra.

Finally, to the best of the authors knowledge there is not report concerning the measurement of carrier transport properties in PS using PT techniques. It is curious that Shen *et al* [98] reported about the existence of a minimum in their measured curves of PA amplitude vs. modulation frequency in PS layers obtained from crystalline p-type Si, which was attributed to carrier recombination effects. These results are quite similar to those obtained by Marín *et al* [50] in p type polycrystalline Si using a similar heat transmission detection configuration, which was attributed by the last authors as due to the carrier recombination effect on the electronic strain signal generation mechanism, as mentioned in Section II. In conclusion, there are several open questions respecting the characterization of PS by photoacoustics.

7. Conclusions and outlook

In this chapter we have tried to give an overview of some applications of the photoacoustic technique in the field of semiconductor thin films characterization, in particular on those related to the measurement of their optical and electronic transport properties, as well as the characterization of their interface with the substrate by means of the measurement of the recombination velocity of the minority photoexcited carriers. The theoretical aspects developed here for particular cases of interest should be extended, with properly modifications, to other experimental situations. Although the first works in this field appeared more than twenty years ago and several papers of research made at laboratory level appear often in the specialized literature, applications of the photothermal methods in the semiconductors industry are unfortunately scarce. The photoacoustic technique should partially fill this lack of applications because several reports indicate their potentialities to allow the access to physical semiconductor properties that are impossible to achieve by conventional techniques in a non-invasive and non-

destructive way. In the case of reduced dimension systems such as those appeared in porous semiconductors, both experimental and theoretical work is impetuous in order to investigate the limits due to the spatial resolution of PAS.

Acknowledgements

The support of SIP-IPN projects 20080032 and 20090160, SEP-CONACyT Grants 61-541 and 83-289 and COFAA-IPN is greatly acknowledged.

References

1. Shroder, D.K. 1990, Semiconductor Material and Device Characterization, Wiley–Interscience, New York.
2. Rosencwaig, A. 1975, Phys. Today, 28, 23.
3. Rosencwaig, A. and Gersho, A. 1976, J. Appl. Phys., 47, 64.
4. Rosencwaig, A. 1990, Photoacoustics and Photoacoustic Spectroscopy, Rober Krieger Publishing Company, Malabar Florida.
5. Mandelis, A. (Ed.) 1987, Photoacoustic and Thermal Wave Phenomena in Semiconductors, Elsevier.
6. Almond, D.P. and Patel, P.M. 1996, “Photothermal Science and Techniques” in “Physics and its Applications, 10”, E.R. Dobbsand and S.B. Palmer (Eds), Chapman and Hall, London.
7. Michell, K., Fahrenbruch, A.L. and Bube, R.H. 1977, J. Appl. Phys., 48, 829.
8. Canham, L.T. 1993, New Scientist (April 10) 23.
9. Mizsei, J. 2007, Thin Solid Films 515, 8310.
10. Petrovsky, A. N., Salnick, A.O., Zuev, V.V., Mukhin, D.O., Mekhtiev, M.M., Pelzl, J., Boccara, A.C. and Fournier, D. 1992, in Photoacoustic and Photothermal Phenomena III, Bicanic, D. (Ed.), Springer Verlag, Berlin-Heidelberg, 396.
11. Chen, Z. H., Bleiss, R. and Mandelis, A. 1993, J. Appl. Phys., 73, 5042.
12. Rosencwaig, A., Opsal, J., Smith, W. L. and Willenborg, D. L. 1985, Appl. Phys. Lett., 46, 1013.
13. Olmstead, M. A. Amer, N. M. Kohn, S. 1983, Appl. Phys. A, 32, 141.
14. Bialkowski, S. E. 1996, “Photothermal Spectroscopic Methods for Chemical Analyses” J. D. Winedorfer (Ed) Wiley, New York.
15. Boccara, A. C. , Fournier, D. and Badoz, J. 1980 Appl. Phys. Lett., 36, 130.
16. Fournier, D., Boccara, C., Skumanich, A. and Amer, N.M. 1986, J. Appl. Phys., 59, 787.
17. Salnick, A., Mandelis, A. and Claude, J. 1996, Appl. Phys. Lett., 69, 2522.
18. Wagner, R.E. and Mandelis, A. 1996, Semicond. Sc. Technol., 11, 289.
19. Wagner, R.E. and Mandelis, A. 1996, Semicond. Sc. Technol., 11, 300.
20. Perondi, L.F., Miranda, L.C.M. 1987, J. Appl. Phys. 62, 2955.

21. Gärtner, W.W. 1960, Phys. Rev. 122, 419.
22. Murphy, J. C. and Aamodt, L.C. 1977, J. Appl. Phys., 48, 3502.
23. Quimby, R.S. and Yen, W.M. 1980, J Appl. Phys., 51, 1780.
24. Quimby, R.S. and Yen, W.M. 1980, J Appl. Phys., 51, 4985.
25. Miranda L.C.M. 1982, Appl. Opt., 21, 2923.
26. Bandeira, J., Cross, H. and Ghizoni, G. 1982 J. Photoacoust. 1, 275.
27. Sablikov, V.A. and Sandomirskii., V.B. 1983, Sov. Phys. Semicond., 17, 50.
28. Sablikov, V.A. and Sandomirskii, V.B. 1983 Phys. Stat. Sol. (b), 120, 471.
29. Gulyaev, Y.V. 1989, Sov. Sci. Rev. A. Phys., 12, 347.
30. Mikoshiba, N., Nakamura, H. and Tsubouchi, K. 1981, in IEEE Ultrasonics Symposium Proceedings, Dallas, Vol. 1, p 443.
31. Jenkins, T.E. 1984, J. Phys. C: Solid State Phys., 17, L799.
32. Dersch, H. and Amer, N. M. 1985 Appl. Phys. Lett., 47, 292.
33. Vargas, H. and Miranda, L.C.M. 1980 Physics Reports, 161, 43.
34. Pinto-Neto, A., Vargas, H., Leite, N.F. and Miranda, L.C.M. 1989, Phys. Rev. B, 40, 3924.
35. Pinto-Neto, A., Vargas, H., Leite, N.F. and Miranda, L.C.M. 1990, Phys. Rev. B, 41, 9971.
36. Nikolic, P.M., Vujatovic, S.S., Todorovic, D.M., Miletic, M.B., Golubovic, A., Bojicic, A.I., Kermendi, F., Duric, S., Radulovic, K.T. and Elazar, J. 1997, Jpn. J. Appl. Phys. , 36, 1006.
37. Dramicanin, M.D., Ristovski, Z.D., Nikolic, P.M., Vasiljevic, D.G. and Todorovic, D.M. 1995, Phys. Rev. B, 51, 14226.
38. Todorovic, D.M., Nikolic, P.M., Vasiljevic, D.G. and Dramicanin, M.D. 1994, J. Appl. Phys. 76, 4012.
39. Todorovic, D.M and Nikolic, P.M. 1997, Opt. Eng., 36, 443.
40. Todorovic, D.M., Nikolic, P.M., Vasiljevic, D.G. and Dramicanin, M.D. 1995, J. Appl. Phys., 78, 5750.
41. Marín, E. Riech, I., Díaz, P., Alvarado-Gil, J. J., Baquero, R., Mendoza-Alvarez, J. G., Vargas, H., Cruz-Orea A. and Vargas, M. 1998 J. Appl. Phys., 83, 2604.
42. Marín, E. Riech, I., Díaz, P., Alvarado-Gil, J. J., Mendoza-Alvarez, J. G., Vargas, H., Cruz-Orea A. and Vargas, M. 1998, Phys. Stat. Sol. (a) 169, 275.
43. Riech, I., Marín, E., Díaz, P., Santana, G., Morales, A. and Vargas, H. 1999, Semicond. Sc. Technol., 14, 543.
44. Riech, I., Díaz, P., Prutskij, T., Mendoza, J., Vargas, H. and Marín, E. 1999, J. Appl. Phys., 86, 6222.
45. Sablikov, V. A. 1987 Sov. Phys. Semicond., 21, 1318.
46. Stearns, R.G. and Kino, G.S. 1985, Appl. Phys. Lett., 47, 1050.
47. Todorovic, D.M, Nikolic, P.M., Bojicic, A.I., Radulovic, K.T. 1997, Phys. Rev. B, 55, 15631.
48. Todorovic, D.M and Nikolic, P.M. 1999 in Progress in Photothermal and Photoacoustic Science and Technology, Optical Engineering Press IV, 271.
49. Todorovic, D.M, Nikolic, P.M. and Bojicic, A.I. 1999, J. Appl. Phys., 85, 7716.
50. Marín, E., Vargas, H., Diaz, P. and Riech, I. 2000, Phys. Stat. Sol.(a) 179, 387.

51. Flaisher, H. and Cahen, D. 1987 in Photoacoustic and Photothermal Phenomena, Hess, P. and Pelzl, J. (Eds.), Springer Verlag, Berlin-Heidelberg, 280.
52. Gusev, V.E. 1987, Akust. Zhurn. (USSR), 33, 223.
53. Gusev, V.E. 1986, Akust. Zhurn. (USSR), 32, 778.
54. Mandelis, A. 1989, J. Appl. Phys., 66, 5572.
55. Mandelis, A., Ward, A. and Lee, K.T. 1989, J. Appl. Phys., 66, 5584.
56. Zhang, Y.L.S. and Cheng, J. 1990, J. Appl. Phys. 68, 1088.
57. Zhang, Y.L.S. and Cheng, J. 1991, Semicond. Sc. Technol., 6, 670.
58. Todorovic, D.M, Nikolic, P.M., Smiljanic, M., Petrovic, R., Bojicic, A.I., Vasiljevic, D.G. and Radulovic, K.T. 1999 in Photoacoustic and Photothermal Phenomena: 10th International Conference, Scudieri, F. and Bertolotti, M. (Eds.), The American Institute of Physics, 503
59. Todorovic, D.M and Smiljanic, M. 2001, Anal. Sc., 17, 291.
60. Rosencwaig, A. 1985 in VLSI Electronics: Microstructure Science, Vol. 9 Einspruch, Ed., Academic Press, Orlando, 227.
61. Cahen, D. and Halle, S.D. 1985, Appl. Phys. Lett., 46, 446.
62. Faria, I.F., Ghizoni, C.C., Miranda, L.C.M. and Vargas, H. 1986, J. Appl. Phys., 59, 3294.
63. Mello, S.M.N., Ghizoni, C.C., Miranda, L.C.M and Vargas, H. 1987, J. Appl. Phys., 61, 5176.
64. Mandelis, A. 1998, Solid-State Electronics, 42, 1.
65. Bell, A. G. 1880, *Am. J. of Sci*. 20, 305.
66. Bell, A.G. and Tainter, S. 1880, *Photophone* United State Patent No. 235, 496.
67. Marquezini, M. V., Cella, N., Manzanares, A. M., Vargas, H. and Miranda, L. C. M. 1991 Meas. Sc. and Techn., 2, 396.
68. Mc. Donald, F. A. and Wetsel, G. C. Jr. 1978 J. of Appl. Phys., 49, 2313.
69. Rousset, G. , Lepoutre, F. and Bertrand, L. 1983 J. of Appl. Phys., 54, 2383.
70. Figielski, T. 1961, Phys. Status. Sol., 1, 386.
71. Delgadillo, I., Vargas, M., Cruz-Orea, A., Alvarado-Gil, J.J., Sánchez-Sinencio, F. and Vargas, H. 1997, Appl. Phys. B, 64, 97.
72. Calderón, A., Muñoz Hernández, R. A., Tomas, S. A., Cruz Orea, A. and Sánchez Sinencio, F. 1998, J. Appl. Phys., 84, 6327.
73. Riech, I., Gomez-Herrera, M. L., Díaz, P., Mendoza-Alvarez, J.G., Herrera-Pérez, J. L. and Marín, E. 2001, Appl. Phys. Lett., 79, 964.
74. Bernal, J., Vargas M., Alvarado, J.J., Delgadillo, I., Cruz, A., Vargas, H., Tufiño, M., Albor, M.L. and González, M.A. 1998, J. Appl. Phys., 83, 3807.
75. González, M.A., Cruz-Orea, A., Albor, M. de L., Castillo, F. de L. 2005, Thin Solid Films, 480–481, 358.
76. Manfredotti, C., Fizzotti, F., Boero, M. and Bossi, Mc. 1996 Solid State Commun., 98, 655.
77. Christofides, C., Engel, A. and Mandelis, A. 1989 Rev. Sci. Instrum., 61, 2360.
78. Vigil-Galán, O., Marín, E., Sastré Hernández, J., Saucedo, E., Ruiz, C. M., Contreras-Puente, G. and Calderón, A. 2007 J. of Mat. Sci., 42, 7176.
79. Ahmed, M. U., Jones, E. D. and Stewart, N. M. 1996, J. Cryst. Growth, 160, 36.
80. Li, J., Xu, Y. F. and Dai, K. 2003 Semicond. Sci. Technol., 18, 611.

81. Vigil-Galán, O., Sastré-Hernández, J., Cruz-Gandarilla, F., Aguilar-Hernández, J., Marín, E., Contreras-Puente, G., Saucedo, E., Ruiz, C.M. and Bermúdez, V. 2006 Sol. Energy Mater. Sol. Cells., 90, 2228.
82. Saucedo, E., Martínes, O., Ruiz, C.M., Vigil-Galán, O., Benito, I., Fornaro, L., Sochinskii, N.V. and Diéguez, E. 2006, J. Cryst. Growth, 291, 416.
83. Vigil-Galán, O., Sánchez-Meza, E., Sastré-Hernández, J., Cruz-Gandarilla, F., Marín, E., Contreras-Puente, G., Saucedo, E., Ruiz, C.M., Tufiño-Velázquez, M. and Calderón, A. 2008, Thin solid films, 516, 3818.
84. Schmuki, P., Lockwood, D.J., Labbé, H.J. y Fraser, J.W. 1996, Appl. Phys. Lett. 69, 1620.
85. Canham, L. T. 1990, Appl. Phys. Lett., 57, 1046.
86. Gupta, A., Jain, V.K., Jalwania, C.R., Singhal, G.K., Arora, O.P., Puri, P.P., Singh, R., Pal, M. and Kumar, V. 1995, Semicond. Sci. Technol., 10, 698.
87. Hummel, R.E., Ludwig, M.H. and Chang, S.S. 1995, Solid State Commun., 93, 237.
88. Hummel, R.E., Ludwig, M., Chang, S.S. and La Torre, G. 1995, Thin Solid Films, 255, 219.
89. Yarkin, D.G., Konstantinova, E.A. and Timoshenko, V.A. 1995, Semiconductors, 29, 348.
90. Brodin, M.S., Blonskii, I.V. and Tkhorik, V.A. 1994, Tech. Phys. Lett., 20, 580.
91. Calderón, A., Alvarado Gil, J. J., Gurevich, Yu. G., Cruz Orea, A., Delgadillo, I., Vargas, H. and Miranda, L. C. M. 1997 Phys. Rev. Lett., 79, 5022.
92. Cruz-Orea, A., Delgadillo, I., Vargas, H., Gudiño-Martínez, A., Marín, E., Vázquez-López, C., Calderón, A. and Alvarado-Gil, J. J. 1996. J. Appl. Phys., 79, 8951.
93. Maxwell, J.C. 1904, A treatise on Electricity and Magnetism, 3rd ed. Oxford University Press, Oxford.
94. Srinivasan, R., Jayachandran, M. and Ramachandran, K. 2007, Cryst. Res. Technol. 42, 266.
95. Blonskij, I. V., Brodyn, M. S., Tkhoryk, V.A., Fillin, A. G. and Piryatinskij, Ju.P. 1997, Semicond.Sci.Technol., 12, 11.
96. Obraztsov, A.N., Okushi, H., Watanabe, H. and Timoshenko, V.Yu. 1997, Phys. Stat. Sol.(b), 203, 565.
97. Ferreira da Silva, A., Souza da Silva, T., Nakamura, O., d'Aguiar Neto, M.M.F., Pepe, I. and Veje, E. 2001, Mat. Res., 4, 23.
98. Shen, Q., Takahashi, T. and Toyoda, T. 2001, Anal. Sciences, 17, 281.